Dual fluid trigeneration combined organic Rankine-compound ejector-multi evaporator vapour compression system

Ali Khalid Shaker Al-Sayyab [a,b], Adrián Mota-Babiloni [a,*], Ángel Barragán-Cervera [a], Joaquín Navarro-Esbrí [a]

[a] ISTENER Research Group, Department of Mechanical Engineering and Construction, Universitat Jaume I, Campus de Riu Sec s/n, 12071 Castelló de la Plana, Spain[1]
[b] Basra Engineering Technical College (BETC), Southern Technical University, Basra, Iraq

A B S T R A C T

This article evaluates the energy and exergy performance of a novel dual fluid combined organic Rankine-compound ejector multi evaporators vapour compression system (ORCEMES) for power, cooling and heating purposes. Six working fluids with ultra-low global warming potential: R1234ze(E), R1243zf, R1234yf for the CEMES and R1234ze(Z), R1336mzz(Z) and R1224yd(Z) for the ORC were selected, resulting in nine combinations. The system can work in two operating modes: power-cooling and power-heating modes. The combination of R1234ze(Z) and R1234ze(E) results in the highest overall system energy performance. The proposed system increases power generation from 21% to 75% at high geothermal and low geothermal temperatures, respectively, compared with separated basic ORC and multi-evaporator systems at the same operating conditions and cooling capacity. The proposed CEMES reduces compressor power consumption to 85% of the basic system, increasing COP remarkably. Concerning the exergy analysis, the low-temperature recapture heat exchanger shows the highest exergy destruction compared to the rest of the components, followed by the turbine. Besides, the second expansion valve presents the lowest exergy destruction percentage.

1. Introduction

During the past century, Anthropogenic greenhouse gas (GHG) emissions have been the predominant cause of the Earth's average temperature increase (Global warming). The burning of fuels for energy production represents the most significant percentage of GHG [1]. Global warming represents one of the most critical challenges humankind has faced in modern times, involving increased global mean surface temperature and the risk of water shortages, increased fire threats, drought, weed, and pest invasions. In 2021, several countries suffered the highest temperature on record. Mediterranean basin countries registered their worst heatwave in over 30 years and a higher number of fires (more than 100 fires in 2021 in Italy, Greece, Turkey, Algeria, and Germany), to name a few warning signs [2].

In October 2014, the European Council achieved an agreement on three higher EU-wide targets that should be attained by 2030: a 40% break in greenhouse gas emissions (compared to 1990 levels), an increase the renewable energy depends by 27%, and a 27% energy saving by higher energy efficiency [3]. In 2019 (39%) of the electricity consumed in the EU was produced by fossil fuel-based power plants [4]. The heating and cooling sector represents 50% of the EU energy demand [5].

Among renewable energy sources, geothermal energy is clean, affordable, environmentally friendly, and cost-effective, with up to 96% capacity factor. Geothermal power plants have only about one-sixth of the natural gas power plants' average CO_2-eq emissions [6].

Today, organic Rankine cycles (ORCs) are a well-known promising low-grade thermal energy recovery technology. However, 80% to 90% of the ORC input heat is released as a lower temperature waste heat to the ambient [7]. Consequently, the electrical efficiency of ORCs is lower than other power cycles, limiting their application [8].

Nomenclature

COP	Coefficient of Performance (-)
E	Expansion (-)
$\dot{Ex}$	Exergy rate (kJ s^{-1})
h	Specific enthalpy (kJ kg^{-1})
$\dot{m}$	Refrigerant mass flow rate (kg s^{-1})
NBP	Normal boiling point (°C)
P	Pressure (bar)
$\dot{Q}$	Heat transfer rate (kW)
s	Entropy (kJ kg^{-1}K^{-1})
T	Temperature (°C)
$\dot{W}$	Power consumption or generation (kW)

Greek symbols

η	Efficiency (-)
ε	Effectiveness
μ	Entrainment ratio
ρ	Density (kg m^{-3})

Subscripts

b	Bulk
C	Compressor, cooling mode
Cri	Critical condition
D	Diffuser, Discharge
Des	Destruction
e	Evaporator
EC	Economic
ej	Ejector
ek	Evaporative condenser
em	Electric-mechanical
exp	Expansion valve
0	Dead state conditions
G	Geothermal
h	Hot stream, heating mode
HT	High temperature
HX	Heat exchanger
HP	Heat pump

in	Inlet
is	Isentropic
II	Second low
K	Condenser
L	Cold stream
LT	Low temperature
M	Mixing
out	Outlet
P	Pump
pn	Primary nozzle
r	Refrigerant, ratio
R	Recapture
sn	Suction nozzle
SD	Super-heating degree
T	Turbine
th	Thermal
v	Volumetric

Abbreviatures

ASHRAE	The American Society of Heating, Refrigerating and Air-Conditioning Engineers
CEMES	Compound Ejector Multi Evaporator System
CO_2-eq	Equivalent carbon dioxide emissions
EES	Engineering Equation Solver
GHG	Greenhouse gas
GWP	Global Warming Potential
HFC	Hydrofluorocarbon
HVAC	Heating Ventilation and Air Conditioning
ODP	Ozone Depletion Potential
ORC	Organic Rankine Cycle
ORCEMES	Organic Rankine Compound Ejector Multi Evaporator System
ORC-VCC	Organic Rankine cycle - vapor compression cycle
LNG	Liquefied Natural Gas
MES	Multi Evaporator System
RORC	Regenerative Organic Rankine Cycle
VCC	Vapour Compression Cycle

Hydrofluorocarbons (HFCs) are greenhouse gases with remarkable global warming potential (GWP), replacing ozone-depleting substances. They are primarily used as working fluids (refrigerants) in HVAC and organic Rankine cycles (ORC). According to the Montreal Protocol, the meeting parties agreed on 15 October 2016 to add HFCs to the list of controlled substances and step down their use by 80% to 85% by the year 2040 [9].

Various low GWP working fluids (refrigerants) have been used recently to increase the ORC performance. For instance, Le et al. [10] performed an ORC energy-exergy comparison with R152a, R32, R744, R1270, R290, R1234yf, and R1234ze(E) as alternatives to R1334a. R32 and R152a were the most efficient energy performance, while R1234ze (E) power generation was the highest.

In 2030, the electricity demands of the European service sector for heating and cooling are expected to increase by 40% compared to that in 2012 [11], contributing to the global mean surface temperature increase. Thus, one of the biggest challenges for the future is producing green electricity and investing in highly efficient cooling systems.

Combined ORC and vapour compression heat pumps (ORC-VCC) have been proposed for individual cooling and power generation or heating and power generation. Aphornratana et al. [12] theoretically concluded for low-grade waste heat recovery that, R22 presents higher performance than R134a, and the liquid-preheater increases the COP. Zhao et al. [13] focused on geothermal energy utilisation. They remarked that the flash pressure, pinch point in the vapour generator, inlet pressure, and ORC turbine back-pressure significantly influences energy performance. Saleh et al. [14] considered several refrigerants for a system powered by low-temperature renewable energy. The condenser represents the highest contribution to the total exergy destruction rate, 34.7%. Liao et al. [15] proposed an ORC-VCC for waste heat recovery from the bottom slag in a coal-fired plant. They highlighted that heptane and cyclohexane are the most convenient refrigerants. Zhar et al. [16] observed that R123 presents the highest ORC energy and exergy efficiency with 6.3 years payback period.

Some studies have shown how various waste heat recovery sources can increase the ORC-VCC efficiency. Lu et al. [17] concluded that butane results in the highest power generation than other working fluids (R600a, R601a, R245fa, R245ca, R236ea), and waste heat recovery increases the energy and exergy efficiency by 37.7% and 35.7%, respectively. Bao et al. [18] compared two different arrangements, ORC-VCC and ORC-flash tank vapour injection cycles, based on single- and dual-fluids (R1270, R290, R161, R152a, R1234yf, and R1234ze(E)). The dual-fluid system with R1234yf-R290 and R290-R152a presents the highest performance and cooling capacity. Including an ejector, Zhu et al. [19] proved that R141b/R134a (55%/45%) achieves an electrical and cooling efficiency of 4.2% and 14.6%, and a COP of 1.1, with an 0.2 optimised entrainment ratio and 351.15 K generator temperature.

In most cases, energy modelling and simulation techniques are combined with exergy analysis. Performance can be optimised by mitigating the sources of thermodynamic irreversibilities in combined ORC-VCC. Akrami et al. [20] proposed tri-generation for power, heating, and hydrogen generation ORC by geothermal energy sources and using the surplus waste heat for domestic hot water. The overall energy and exergy efficiencies were 26.1% and 44.5%, respectively, with 43.5 kW net power and 149.8 kW heating generation, associated with 0.2 kg h^{-1} of pure hydrogen produced. Boyaghchi et al. [21] simulated an ORC-VCC driven by solar-geothermal energy and improved the R134a, R423A, R1234yf, and R1234ze(E) with water/CuO nanofluid. R134a presents the highest exergy performance, while from an exergoeconomic and exergoenvironmental perspective, R1234yf presents the best results. Li et al. [22] evaluated energy and exergy performance for the combined CO_2 power cycle-absorption chiller and gas turbine waste heat recovery. The combination presented exergy efficiency increase by 2.9% and 1.3%. Nasir et al. [23] modelled a small-scale biomass-powered ORC-VCC for trigeneration. The boiler saturation temperature increases the heat capacity rate and reduces the overall exergy destruction.

Different waste heat configurations could benefit the overall ORC performance. Teng et al. [24] compared three ORC arrangements for power-heating purposes: serial, condensation, and compound. The serial system presented the highest thermal and exergy efficiency, whereas the combination highlighted economic performance. Aliahmadi et al. [25] compared three arrangements of geothermal-based ORC: basic ORC, RORC, and two thermoelectric generators. ORC with two thermoelectric generators shows the highest exergy, energy efficiency, and power generation. Meng et al. [8] compared the flash-ORC cycle and two-stage ORC using R600, R600a, R6001, R601a, and R1234ze(E). A higher heat source temperature benefits thermodynamic and techno-economic performance, showing the R601 flash-ORC system the highest values.

In the light of previous studies, there is a vast interest in trigeneration power, cooling, and heating from ORC-VCC systems. All ORC-VCC combinations mentioned in the previous literature focused on system performance-enhancing by the ORC generated power increase without accounting for VCC performance augmentation. However, a proven research gap in ORC-VCC systems powered by geothermal energy and VCC improved through additional heat exchangers and ejectors. The main objective of the work is to investigate two different configurations of dual fluid combined ORC and compound ejector multi evaporator vapour compression cycle from an energy and exergy efficiency point of view to protect the environment. All proposed configurations have not been studied before as potential dual fluid trigeneration cycles (multi evaporator two cooling levels, heating, and power generation).

The organic Rankine-compound ejector multi evaporator vapour compression system (ORCEMES) adopts two different methods to increase the overall thermal-economic performance: compound ejector multi evaporator vapour compression system (CEMES) and CEMES condenser waste heat utilisation for variable geothermal heat source

temperature. The CEMES condenser waste heat increases the ORC generated electricity. Besides, the ejector improves the CEMES performance, where a geothermal heat source is used. The heat of the geothermal source recovered by ORCEMES is used for power generation and provides heating for fulfilling the entire building and greenhouse demands. Besides, the chilled water is produced from two evaporator levels to overcome the building and greenhouse demand. A sensitivity analysis was conducted to investigate the effects of three temperatures: geothermal, ORCEMES condensing and greenhouse.

The heat pump condenser waste heat is utilised to increase the ORC power generation at low-grade geothermal heat temperature in the power-cooling mode. The surplus geothermal waste heat from the ORC evaporator is used directly for heating purposes in the power-heating mode. Environmentally friendly refrigerants R1234ze(E), R1243zf, R1234yf (for CEMES), R1234ze(Z), R1336mzz(Z) and R1224yd(Z) (for ORC) are considered in the ORCEMES for power-heating and cooling applications.

The main contributions of the present work are the proposal of a novel dual fluid combined ORC-compound ejector-multi evaporator vapour compression system (ORCEMES) for power-cooling, and power-heating purposes, using low GWP refrigerants and condenser waste heat utilisation for performance increase; evaluation of the system feasibility in two modes at different geothermal heat supply temperatures. The system models are developed in Engineering Equation Solver (EES) software.

2. System description

2.1. Configurations

The system is composed of an ORC combined with a compound greenhouse waste heat-driven ejector-multi evaporator VCC, which can operate in power-cooling and power-heating modes, utilising a geothermal heat source for power generation.

The first arrangement is proposed for cooling demands in the combined power-cooling mode (Fig. 1.a). The system includes two main cycles: the first is the power generation cycle (ORC), in which the main components are an evaporator, turbine, condenser, HT recapture heat exchanger, and pump. The second one is the compound ejector-multi evaporator vapour compression system (CEMES), composed of an ejector, compressor, high and low-temperature evaporators (two cooling levels), separator tank, and heat exchanger condenser waste heat recovery (LT recapture). The system uses the CEMES condenser waste heat to increase the ORC performance while using greenhouse waste heat absorbed by the high-temperature level evaporator as an ejector-driven force to operate the system with a higher COP. The system absorbs heat from a geothermal source to produce power and cooling at two levels (building air conditioning and greenhouse cooling). The low boiling temperature refrigerants are used for CEMES, whereas the higher ones are used for the ORC. There is no mass transfer between both cycles, so the combination occurs in the CEMES condenser.

Then, in the combined power-heating mode (Fig. 1.b), the system comprises only one ORC with building and greenhouse heat exchangers. In this configuration, when the geothermal supply temperature is below 65 °C, the geothermal water is used directly for heating only, with no power generation. In contrast, when the geothermal supply temperature exceeds 65 °C, the system generates power and uses the surplus geothermal waste heat directly from the ORC evaporator outlet for heating. Hence, this arrangement uses condenser waste heat for greenhouse heating instead of rejecting it to the ambient (reducing the power consumption by the absence of the cooling tower).
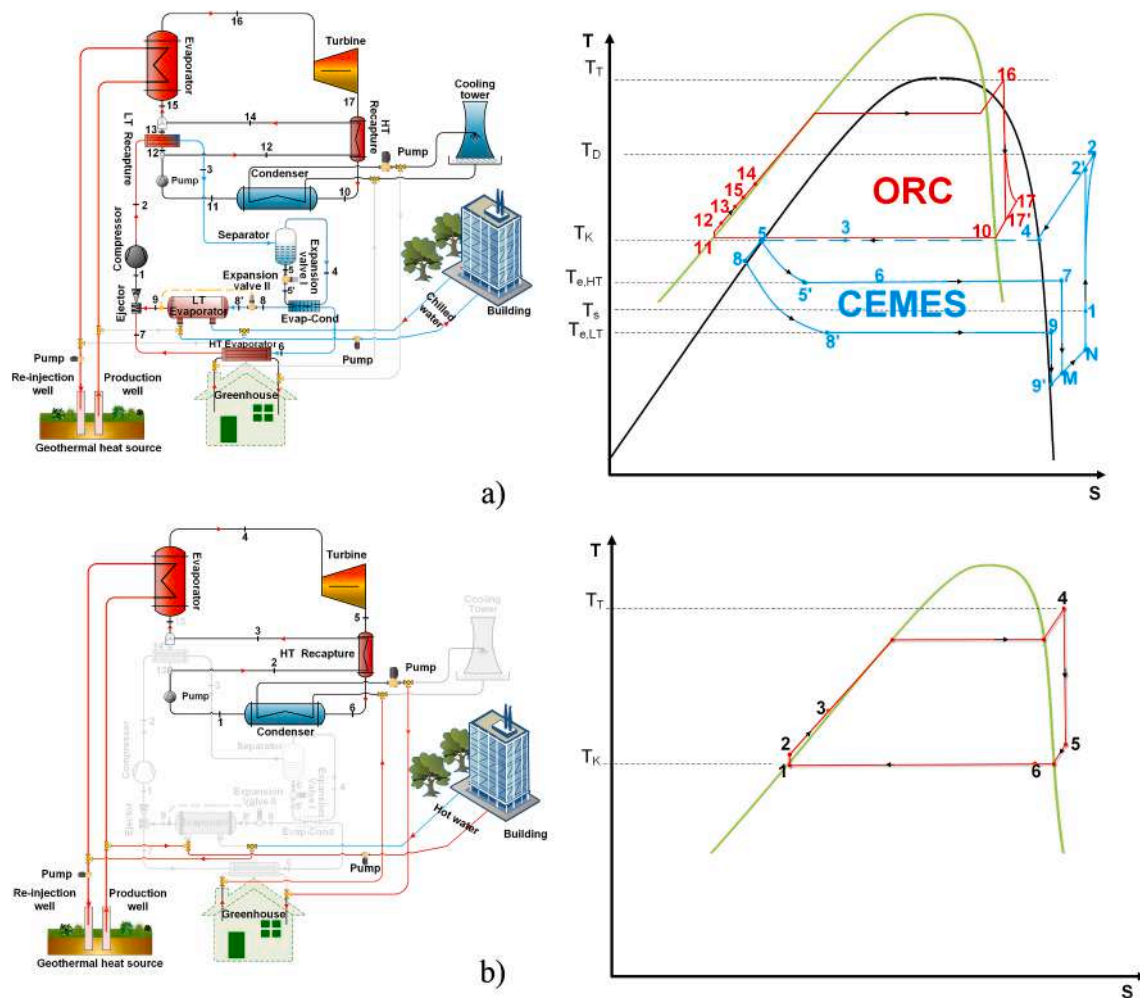
Fig. 1. Schematic and P-h diagram of proposed modes: a) combined power-cooling (ORCEMES), and b) combined power-heating.

2.2. Working fluids

HFCs are greenhouse gases that contribute to global warming up to hundreds or thousands of times more than carbon dioxide (CO_2). In 2050, the HFCs consumption and production should be pended according to Kigali Amendment to the Montreal Protocol.

R245fa is an HFC refrigerant widely used in ORC units, with a GWP value of 1030. Besides that, R134a has been one of the refrigerants most commonly used in refrigeration and air conditioning applications, with a GWP value of 1430. The current study considers six environmentally friendly refrigerants; R1234ze(Z), R1336mzz(Z) and R1224yd(Z) for ORC, and R1234ze(E), R1243zf, R1234yf for CEMES. They all present ultra-low GWP (below 8) and comparable energy-exergy performance [26]. Nine refrigerant pairs are generated due to the combination of the proposed refrigerants.

Table 1 presents their main properties. It is necessary to conduct an in-depth assessment to determine the most convenient combination for the proposed system.

Table 1
Main properties of selected refrigerants [27,28].

Refrigerants	Molecular weight (g mol^{-1})	T_{crit} (°C)	P_{crit} (bar)	NBP (°C)	ρ (kg m^{-3})	h_{fg} (kJ kg^{-1})	ODP	GWP$_{100}$	Safety class ASHRAE
R1234ze(E)	114.0	109.4	36.32	−19.28	5.71	195.6	0	7	A2L
R1234yf	114.0	94.7	33.82	−29.49	5.98	180.2	0	4	A2L
R1243zf	96.05	103.8	35.18	−25.43	4.95	217.2	0	1	A2L
R1234ze(Z)	114	150.1	35.3	9.8	5.101	204.7	0	6	A2L
R1336mzz(Z)	164.1	171.3	29.0	33.45	6.833	170.74	0	2	A1
R1224yd(Z)	148.5	155.5	33.4	14.6	6.598	166.35	0.00023	0.88	A1

*At a pressure of 1.01325 bar.

3. Methodology

3.1. System modelling

The proposed system is modelled using EES (Engineering Equation Solver) software [27], where all assumptions, boundary conditions, and inputs are introduced. The methodology flow chart for calculating the energy-exergy performance of ORCEMES in different scenarios and modes is shown in Fig. 2.
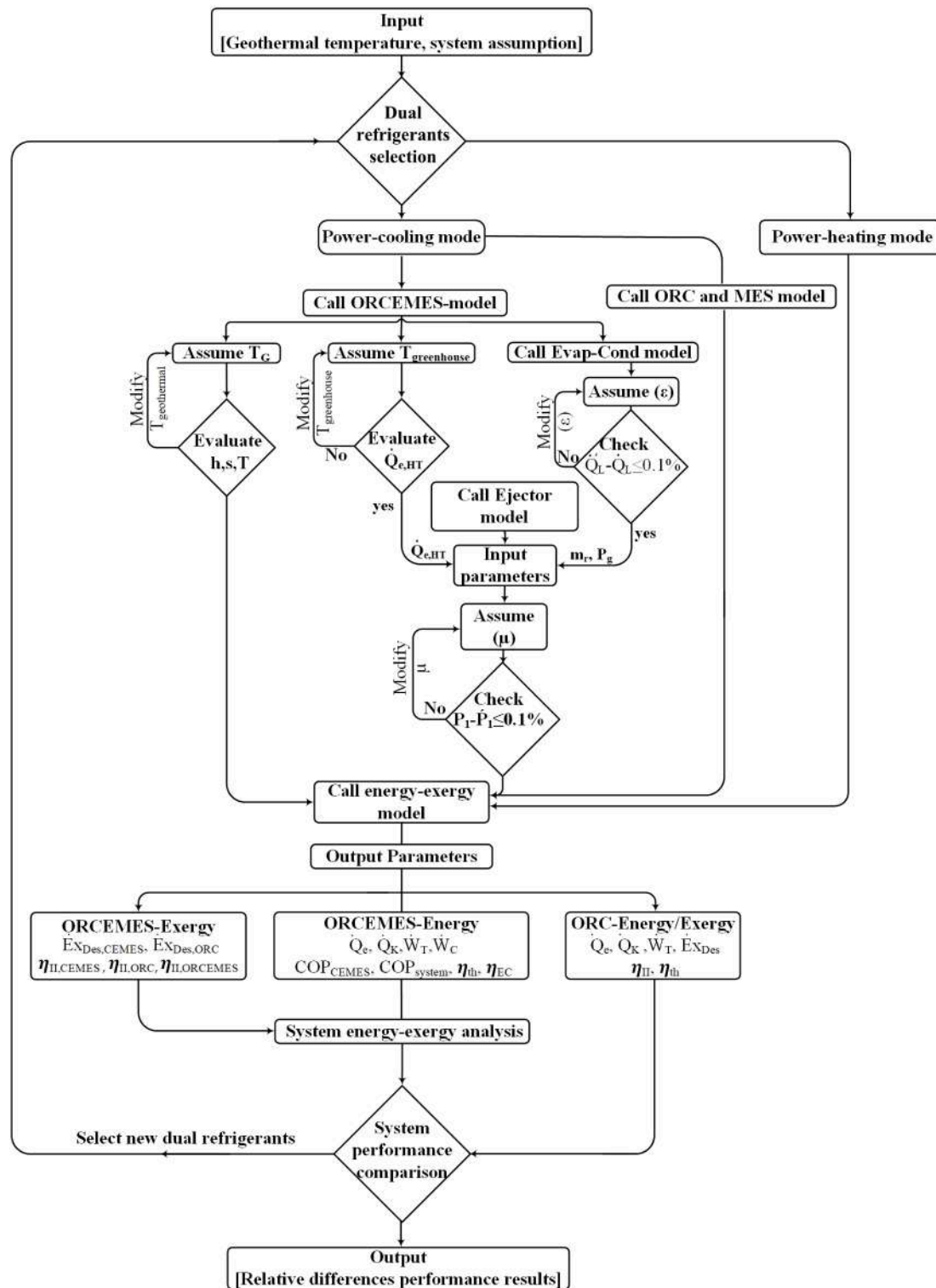

Fig. 2. Methodology flow chart.

Table 2

Assumptions and boundary conditions.

Parameters	Assumed value
ORCEMES condensing temperature	25 to 35 °C
CEMES condensing temperature	30 to 45 °C
LT evaporator temperature	2 °C
$\Delta T_{cooling\ media}$	5 °C
T_0 (heating, cooling)	283 K, 298 K
Cooling load	120 kW
Greenhouse temperature	30 to 40 °C
Geothermal supply temperature	55 to 90 °C [29]
$\dot{m}_G$	7.5 kg s^{-1}
$\dot{m}_r$	11 kg s^{-1}
η_P	70% [30]
η_{pn}	90% [31]
η_{sn}	95% [19]
η_D and η_m	85% [26]
ε_{HX}	80% [32]
η_{em}	88% [33]
$\eta_{is,C}$	85% [34]
$\eta_{is,T}$	80% [30]

3.2. Boundary conditions and assumptions

The geothermal supply temperature ranged from 55 to 90 °C to evaluate the system performance under different conditions. In the same context, in the power-cooling mode, the ORC condensing temperature varied from 25 to 35 °C; the CEMES condensing temperature ranged from 30 to 45 °C. A constant cooling load of 120 kW was considered for all operating conditions, with a 2 °C evaporating temperature (low-temperature evaporator). The temperature varied from 30 to 40 °C to study the effect of greenhouse inlet temperature on system performance. Pressure drops and heat transfer losses are neglected through the connection pipes and across the compressor. Table 2 contains the main assumptions and boundary conditions.

3.3. Equations

3.3.1. Energy model

The energy and mass conservation laws are adopted to evaluate the system's performance. The main energy and mass balance equations for the system components are given in Table 3. The ejector model is mentioned in detail by Al-Sayyab et al. [26].

The overall system performance comes from separated CEMES and ORC subsystems evaluation. For the heat pump, the performance is indicated by the coefficient of performance (COP), and it can be obtained through Eq. (1).

$$COP_C = \frac{\dot{Q}_e}{\dot{W}_C} \tag{1}$$

Where $\dot{Q}_e$: Is the cooling capacity summation of the low and high-temperature evaporators.

For the ORC, the thermal efficiency performance is determined by Eq. (2).

$$\eta_{th} = \frac{\dot{W}_{net}}{\dot{Q}_{in}} \tag{2}$$

In the power-cooling mode, Eq. (3) and (4) are used, whereas in the power-heating mode, Eq. (5) and (6).

$$\dot{W}_{net} = \dot{W}_T - \dot{W}_P - \dot{W}_C \tag{3}$$

$$\dot{Q}_{in} = \dot{Q}_{e,ORC} + \dot{Q}_{R,LT} \tag{4}$$

$$\dot{W}_{net} = \dot{W}_T - \dot{W}_P \tag{5}$$

$$\dot{Q}_{in} = \dot{Q}_{e,ORC} \tag{6}$$

Finally, the overall system performance can be evaluated using Eq. (7).

$$COP_{system} = COP\ \eta_{th} \tag{7}$$

3.3.2. Exergy model

The source of thermodynamic inefficiencies due to the components' irreversibility is also determined. The exergy analysis indicates a thermodynamic system's ability to use the available energy. Dead state conditions are taken as ambient temperature and pressure. The nominal exergy balance equation can be written as indicated in Eq. (8) and (9) [35].

$$0 = \left(1 - \frac{T_0}{T_b}\right)\dot{Q} - \dot{W} + \dot{Ex}_{in} - \dot{Ex}_{out} - \dot{Ex}_{Des} \tag{8}$$

$$\dot{Ex} = \dot{m}(h - h_0 - T_0(s - s_0)) \tag{9}$$

Where temperatures are expressed in K.

Table 4

Exergy destruction rate equations for ORCEMES components [35,37,38].

Component	Exergy Equation
Pump	$\dot{Ex}_{Des,P} = \dot{Ex}_{in} - \dot{Ex}_{out} + \dot{W}_P$
LT Recapture	$\dot{Ex}_{Des,R,HT} = (\dot{Ex}_{in} - \dot{Ex}_{out})_{r,ORC} + (\dot{Ex}_{in} - \dot{Ex}_{out})_{r,HP}$
HT Recapture	$\dot{Ex}_{Des,R,LT} = (\dot{Ex}_{in} - \dot{Ex}_{out})_{r,l} + (\dot{Ex}_{in} - \dot{Ex}_{out})_{r,h}$
Mixing	$\dot{Ex}_{Des,M,ORC} = \dot{Ex}_{in} - \dot{Ex}_{out}$
ORC Evaporator	$\dot{Ex}_{Des,e,ORC} = (\dot{Ex}_{in} - \dot{Ex}_{out})_r + (\dot{Ex}_{in} - \dot{Ex}_{out})_G$
Turbine	$\dot{Ex}_{Des,T} = \dot{Ex}_{in} - \dot{Ex}_{out} - \dot{W}_T$
ORC Condenser	$\dot{Ex}_{Des,K,ORC} = (\dot{Ex}_{in} - \dot{Ex}_{out})_r + (\dot{Ex}_{in} - \dot{Ex}_{out})_w$
Compressor	$\dot{Ex}_{Des,C} = \dot{Ex}_{in} - \dot{Ex}_{out} + \dot{W}_C$
Condenser	$\dot{Ex}_{Des,K} = (\dot{Ex}_{in} - \dot{Ex}_{out})_r + (\dot{Ex}_{in} - \dot{Ex}_{out})_w$
Evaporative-Condenser	$\dot{Ex}_{Des,ek} = (\dot{Ex}_{in} - \dot{Ex}_{out})_{r,l} + (\dot{Ex}_{in} - \dot{Ex}_{out})_{r,h}$
HT Evaporator	$\dot{Ex}_{Des,e,HT} = (\dot{Ex}_{in} - \dot{Ex}_{out})_r + (\dot{Ex}_{in} - \dot{Ex}_{out})_w$
Ejector	$\dot{Ex}_{Des,ej} = \dot{Ex}_{in} - \dot{Ex}_{out}$
Expansion valve	$\dot{Ex}_{Des,exp} = \dot{Ex}_{in} - \dot{Ex}_{out}$
LT Evaporator	$\dot{Ex}_{Des,e,LT} = (\dot{Ex}_{in} - \dot{Ex}_{out})_r + (\dot{Ex}_{in} - \dot{Ex}_{out})_w$

Table 3

Energy and mass balance equations.

Components	Energy balance equations		Mass balance
	Power-cooling mode	Power-heating mode	
Pump	$\dot{W}_P = \dot{m}_{r,ORC}(h_{12} - h_{11})$	$\dot{W}_P = \dot{m}_r(h_2 - h_1)$	–
LT Recapture	$\dot{Q}_{R,LT} = \dot{m}_{13}(h_{13} - h_{12}) = \dot{m}_1(h_2 - h_3)$	–	–
HT Recapture	$\dot{Q}_{R,HT} = \dot{m}_{r,ORC}(h_{17} - h_{10}) = \dot{m}_{r,14}(h_{14} - h_{12})$	$\dot{Q}_{R,HT} = \dot{m}_r(h_3 - h_2) = \dot{m}_r(h_5 - h_6)$	–
Mixing tank	$\dot{m}_{r,ORC}h_{15} = \dot{m}_{13}h_{13} + \dot{m}_{14}h_{14}$	–	$\dot{m}_{r,ORC} = \dot{m}_{13} + \dot{m}_{14}$
ORC evaporator	$\dot{Q}_{e,ORC} = \dot{m}_{r,ORC}(h_{16} - h_{15}) = \dot{m}_G(h_{in} - h_{out})$	$\dot{Q}_{e,ORC} = \dot{m}_r(h_4 - h_3) = \dot{m}_G(h_{in} - h_{out})$	–
Turbine	$\dot{W}_T = \dot{m}_{r,ORC}(h_{16} - h_{17})$	$\dot{W}_T = \dot{m}_r(h_4 - h_5)$	–
ORC Condenser	$\dot{Q}_{K,ORC} = \dot{m}_{r,ORC}(h_{10} - h_{11})$	$\dot{Q}_{K,ORC} = \dot{m}_r(h_6 - h_1)$	–
Compressor	$\dot{W}_C = \dot{m}_1(h_2 - h_1)$	–	–
LT Evaporator	$\dot{Q}_{e,LT} = \dot{m}_5(h_9 - h_{8'})$	–	–
HT Evaporator	$\dot{Q}_{e,HT} = \dot{m}_4(h_7 - h_6)$	–	–
Separator	$\dot{m}_1 h_3 = \dot{m}_4 h_4 + \dot{m}_5 h_5$	–	$\dot{m}_1 = \dot{m}_4 + \dot{m}_5$

Table 4 lists the rate of exergy destruction equations for each ORCEMES component.

Also, the total exergy destruction for all CEMES components is evaluated by Eq. (10).

$$\dot{Ex}_{Des,CEMES} = \dot{Ex}_{Des,C} + \dot{Ex}_{Des,R,LT} + \dot{Ex}_{Des,LT,e} + \dot{Ex}_{Des,ej} + \dot{Ex}_{Des,exp} + \dot{Ex}_{Des,HT,e}$$

(10)

The exergy efficiency of the CEMES is calculated using Eq. (11).

$$\eta_{II,CEMES} = 1 - \frac{\dot{Ex}_{Des,CEMES}}{\dot{Ex}_{in}}$$

(11)

In the same context, the total exergy destruction for all ORC components is obtained by Eq. (12).

$$\dot{Ex}_{Des,ORC} = \dot{Ex}_{Des,T} + \dot{Ex}_{Des,K,ORC} + \dot{Ex}_{Des,e,ORC} + \dot{Ex}_{Des,P,ORC} + \dot{Ex}_{Des,R,HT} + \dot{Ex}_{Des,M,ORC}$$

(12)

The system's economic efficiency can be evaluated using the metrics indicated in Eq. (15) for the combined power-cooling mode and Eq. (16) for the combined power-heating mode [36].

$$\eta_{EC,C} = \frac{\dot{W}_{net} + 0.8\dot{Q}_{e,CEMES}}{\dot{Q}_{e,ORC}}$$

(15)

$$\eta_{EC,H} = \frac{\dot{W}_{net} + 0.5\dot{Q}_{K,ORC}}{\dot{Q}_{e,ORC}}$$

(16)

4. Results and discussion

4.1. Combined power-cooling mode

4.1.1. Dual working fluids selection

In addition to a higher overall thermal efficiency, ORCEMES should be based on working fluids matching environmental requirements (zero ODP and low GWP), safety and low cost. The current study considers six environmentally friendly refrigerants, R1234ze(E), R1243zf, R1234yf (for CEMES), R1234ze(Z) R1336mzz(Z), and R1224yd(Z) (for ORC) that, when combined, result in nine pairs.

The average overall COP and net power generating are taken as a figure of merit to select suitable refrigerants pair with a high ORCEMES thermal efficiency and COP. Fig. 3 depicts all investigated refrigerants pairs. The pair R1234ze(Z)-R1234ze(E) provides the highest average overall system COP associated with the highest generating power. Therefore, it is selected as the working fluid pair used for the rest of the article.

4.1.2. Geothermal supply temperature influence on system performance

In the light of the previous section, a sensitivity analysis is adopted for the pair R1234ze(Z)-R1234ze(E). Fig. 4.a evidences that in the power-cooling mode, both the ORC evaporator capacity and turbine-power generation are directly proportional to the geothermal supply temperature, owing to a geothermal capacity increase.

In the same context, the geothermal supply temperature variation does not affect the compound ejector-multi evaporator system performance while benefiting the net power generation. Hence, thermal efficiency increases (Fig. 4.c) due to turbine power generation augmentation at constant pressure and pump power consumption.

On the other hand, a higher ORC condenser temperature reduces the turbine power generated due to the expansion ratio decreasing (Fig. 4.b). Both net power and thermal efficiency decrease in turbine power generation decrease with constant compressor consumption power (Fig. 4.a).

Finally, the increase in geothermal supply temperature positively influences the ORCEMES COP (Fig. 4.d) owing to the rise in power generation and thermal efficiency (Fig. 4.c). On the other hand, when the ORC's condensing temperature increases, the ORCEMES COP decreases at a given geothermal supply temperature due to the power generation reduction (thermal efficiency decreases at a given geothermal supply temperature, Fig. 4.c). In addition, due to the increase in power generated with geothermal temperature, thermoeconomic efficiency is benefitted Fig. 4.d—finally, the highest ORCEMES system COP and thermoeconomic efficiency result at the lowest ORC condensing temperature considered, 25 °C.
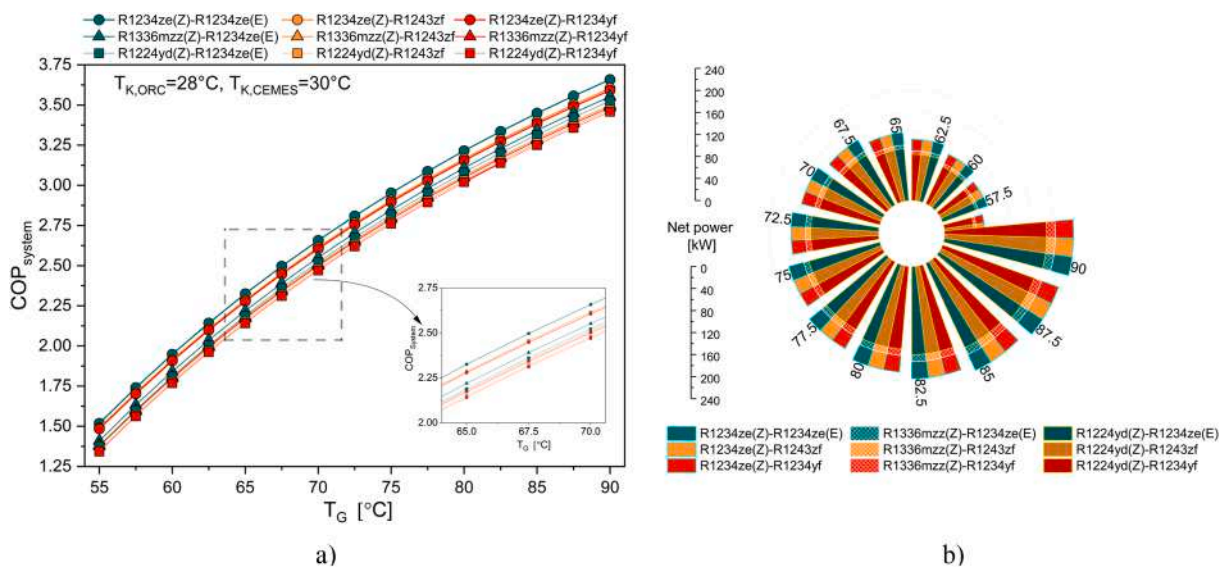

Fig. 3. Geothermal supply temperature variation for different refrigerants pairs: a) system COP and b) net power.
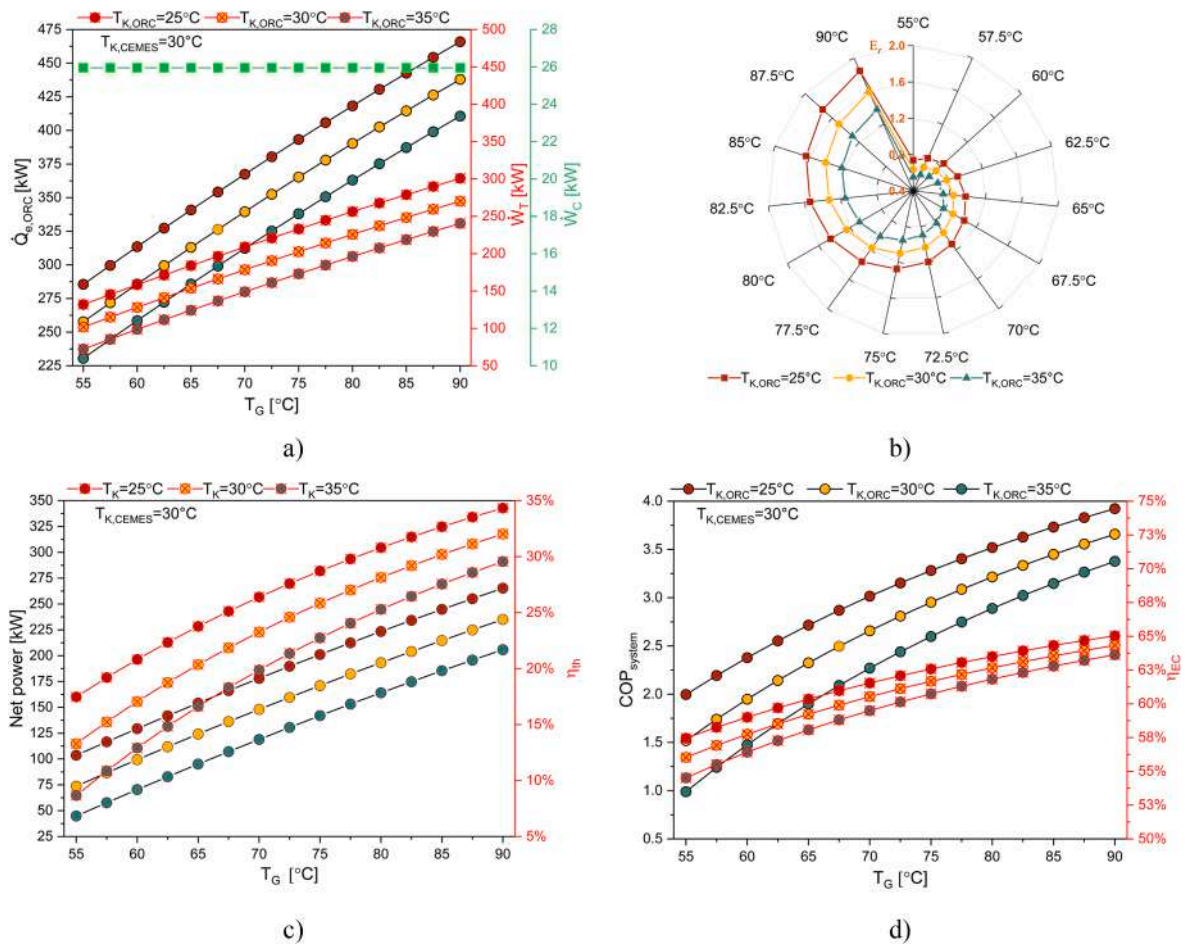
a)

b)

c)

d)

Fig. 4. Effect of geothermal supply temperature at different ORC condensing temperatures on a) power generation, evaporator capacity and power consumption, b) turbine expansion ratio, c) net power generation and thermal efficiency, and d) overall system COP and thermal-economic efficiency.

4.1.3. CEMES condensing temperature effect on system performance

Due to the compressor pressure ratio increase with CEMES's condensing temperature increase (Fig. 5.a), the compressor power consumption increases (Fig. 5.b). Besides overcoming the reduction in the condenser heat rejection, the refrigerant mass flow rate is incremented, Fig. 5.a. Similarly, all these factors led to an adverse effect of the condensing temperature on the CEMES COP due to increased compressor consumption. In the aftermath, the system COP, thermoeconomic efficiency, and thermal efficiency were decreased (Fig. 5.c) with the CEMES's condensing temperature increasing.

4.1.4. Greenhouse temperature influence on system performance

The currently proposed system uses waste heat generated by the greenhouse plants as the ejector driving force. The current combination of ejector and compressor reduces the compressor pressure ratio with the increase of the greenhouse temperature (Fig. 6.a) as the pressure supplied by the ejector increases. The refrigerant mass flow rate decreases due to the super-heating degree increase (Fig. 6.a) with the cooling load requirement reduction. Furthermore, this behaviour reduces compressor power consumption (Fig. 6.b) for the condensing and geothermal supply temperatures.

The greenhouse temperature increase modestly affects the ORCEMES net power generation and thermal efficiency for geothermal, low evaporator temperature and condensers conditions (Fig. 6.b). Likewise, the overall system COP (Fig. 6.c). After all, the economic efficiency slightly increases with the greenhouse temperature, owing to a modest effect on power consumption (Fig. 6.c).

4.1.5. Exergy analysis

The ORCEMES exergy performance at different geothermal supply temperatures and fixed condensing and evaporating temperatures is investigated in this section. From Fig. 7, it is evidenced that the low -temperature recapture heat exchanger represents the largest source of exergy destruction in the whole system, followed by the turbine and ejector (45.4%, 27% and 7.2%, respectively). The high-temperature recapture heat exchanger, the second expansion valve, and pump contribution to the exergy destruction percentage are negligible (below 1%).

The exergy efficiency was directly proportional to the geothermal supply temperature increase (Fig. 8.a) due to minor total exergy destruction compared to the total exergy input. The contrary happens to CEMES; the exergy performance of CEMES is not affected by the geothermal supply temperature.
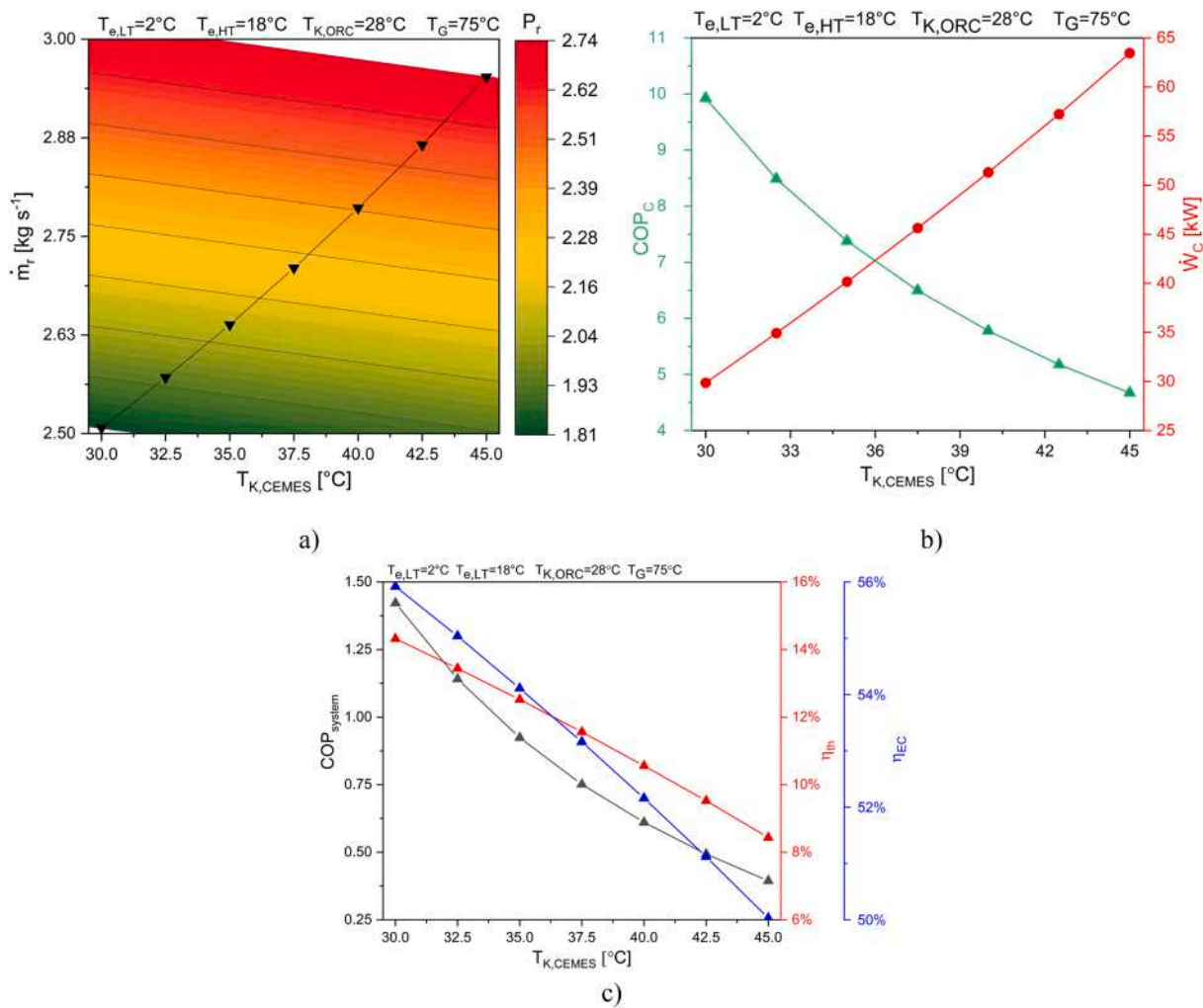

Fig. 5. Effect of CEMES condensing temperatures on: a) refrigerant mass flow rate, b) CEMES COP, consumption power and c) overall system COP, thermal efficiency and economic efficiency.
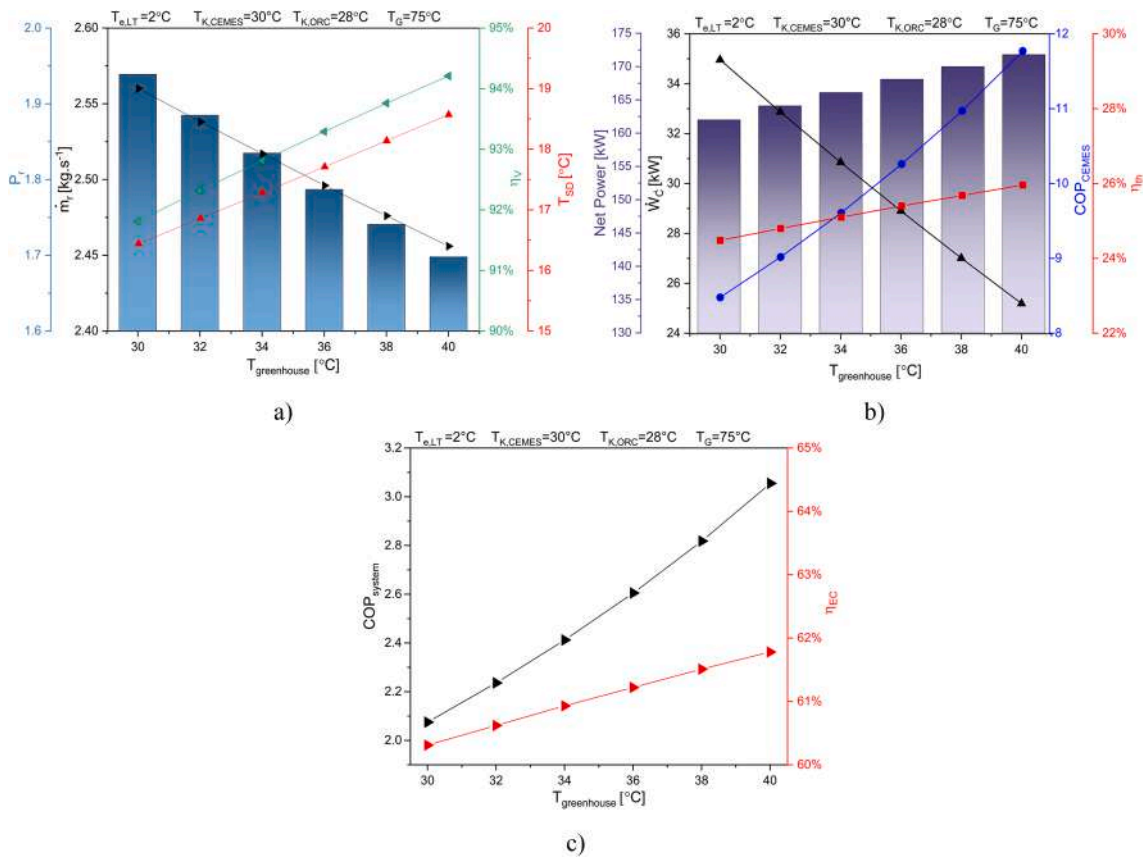
Fig. 6. Effect of greenhouse temperature on a) refrigerant mass flow rate, b) power consumption and c) system COP and thermal economic efficiency.
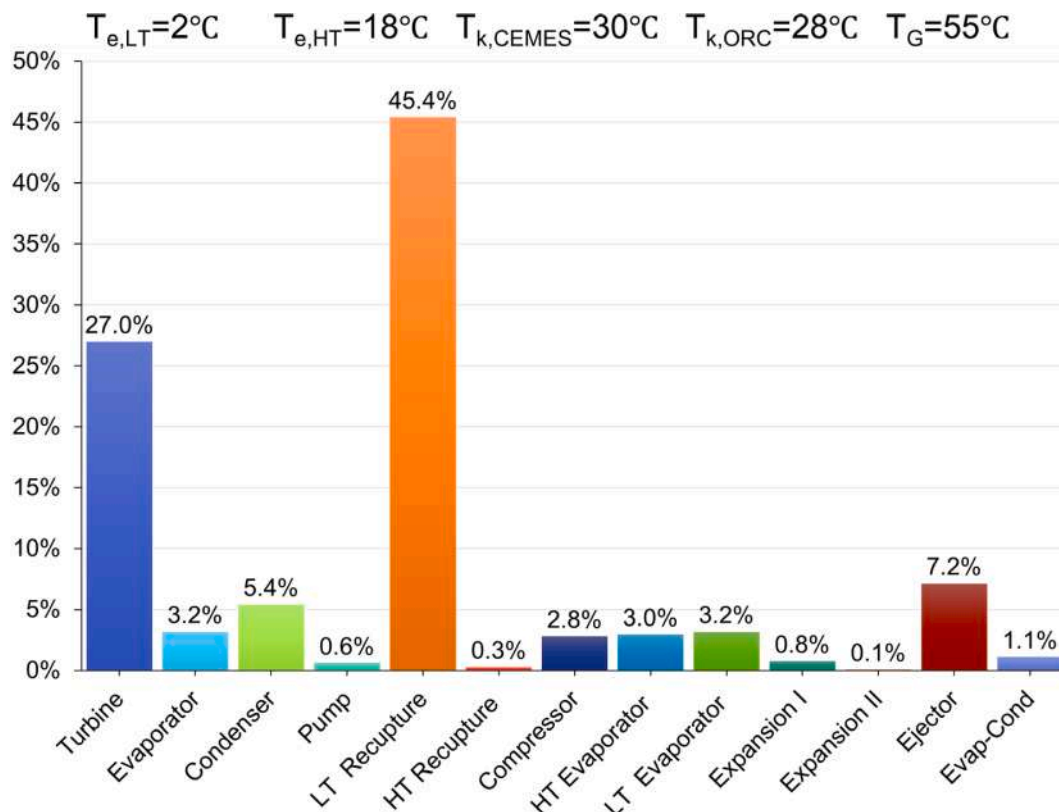

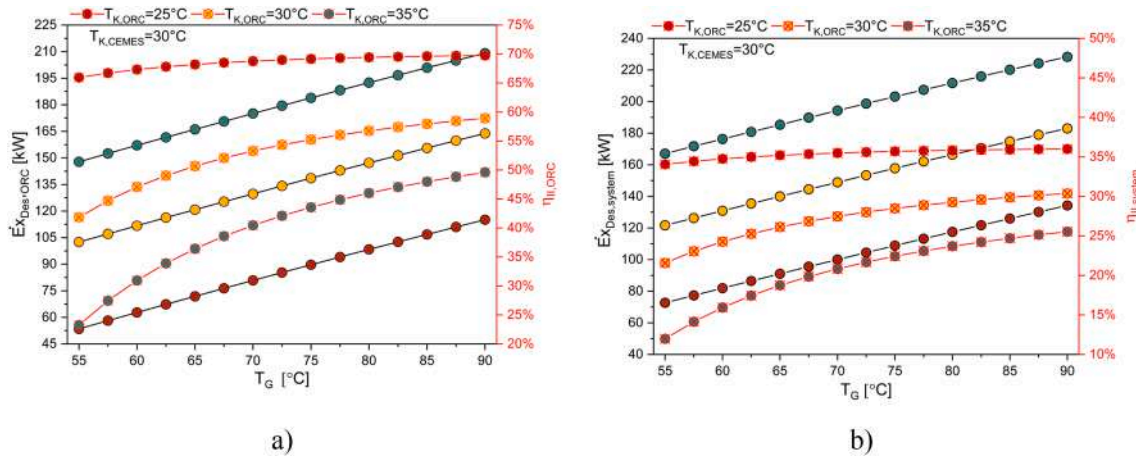Fig. 7. ORCEMES relative exergy destruction by component.

Fig. 8. Effect of geothermal supply temperature on exergy performance of a) ORC and b) ORCEMES.

The ORC condenser temperature increase enormously decreases exergy performance due to the turbine exergy destruction increase, expansion ratio decrease (Fig. 4.b), and a higher temperature difference across evaporator and condenser. It does not affect CEMES exergy destruction. In the aftermath of the above, the ORCEMES overall exergy performance follows sub-cycles behaviour (ORC), Fig. 8.b. The highest overall system exergy efficiency is observed at the lowest ORC condenser temperature considered in this work, 25 °C.

In the same context, an increase in CEMES condenser temperature significantly impacts the exergy efficiency due to the compressor exergy destruction increase, pressure ratio increase (Fig. 5.a), and the higher temperature difference across evaporator condenser and evaporative-condenser. All these factors led to the ORCEMES's overall exergy performance following CEMES behaviour, Fig. 9. The highest ORCEMES exergy efficiency is observed at 30 °C CEMES condensing temperature.

From Fig. 10, it is extracted that the greenhouse temperature increase benefits the CEMES exergy performance only due to the decreasing power consumption (Fig. 6.b) and the decreasing

temperature difference across the second evaporator and evaporative-condenser. It does not affect the ORC exergy performance, which slightly increases the overall system exergy efficiency.

4.2. Combined power-heating mode

When the geothermal supply temperature is around 65 °C, geothermal water is used directly for building heating without power generation. Moreover, the full power-heating mode works when the geothermal supply temperature exceeds 65 °C. After being applied to the ORC evaporator, the system uses surplus geothermal heat for heating purposes.

As shown in Fig. 11.a, a higher geothermal supply temperature increases power generation and thermal economic efficiency due to the augmentation of evaporator heating. Fig. 11.b shows the geothermal supply temperature's influence on exergy performance. The geothermal supply temperature slightly increases the exergy efficiency due to higher exergy destruction.
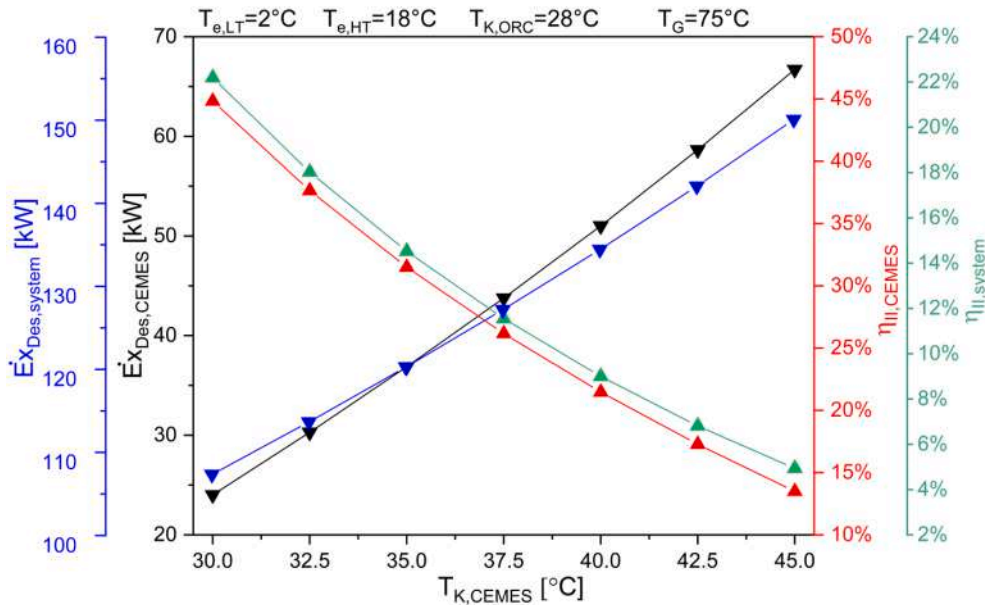

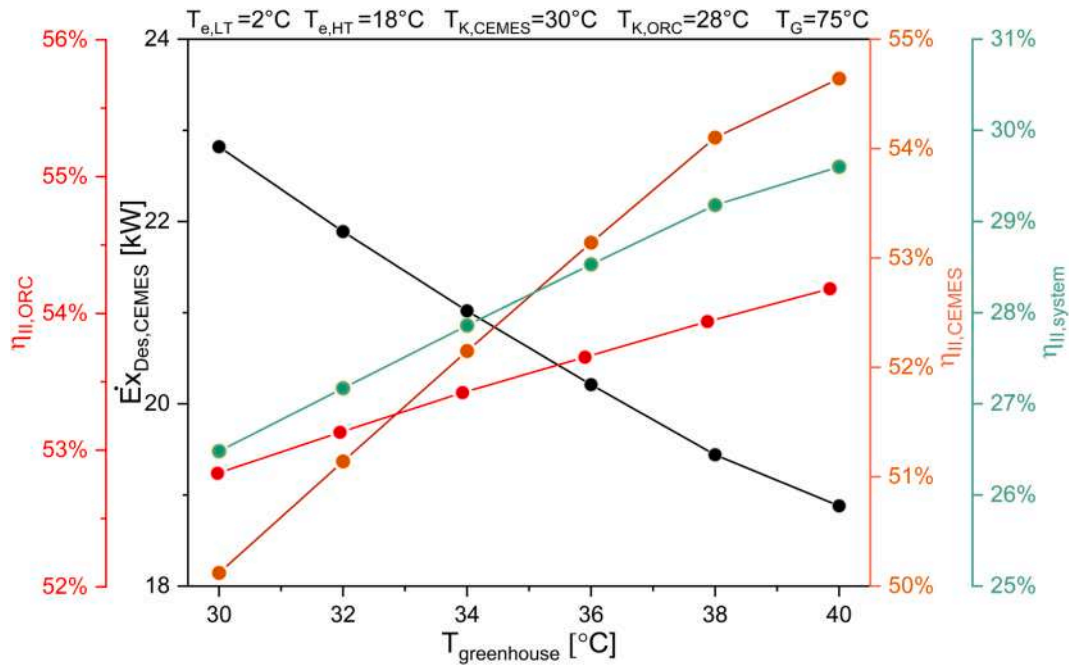**Fig. 9.** Effect of CEMES condenser temperature on exergy performance.

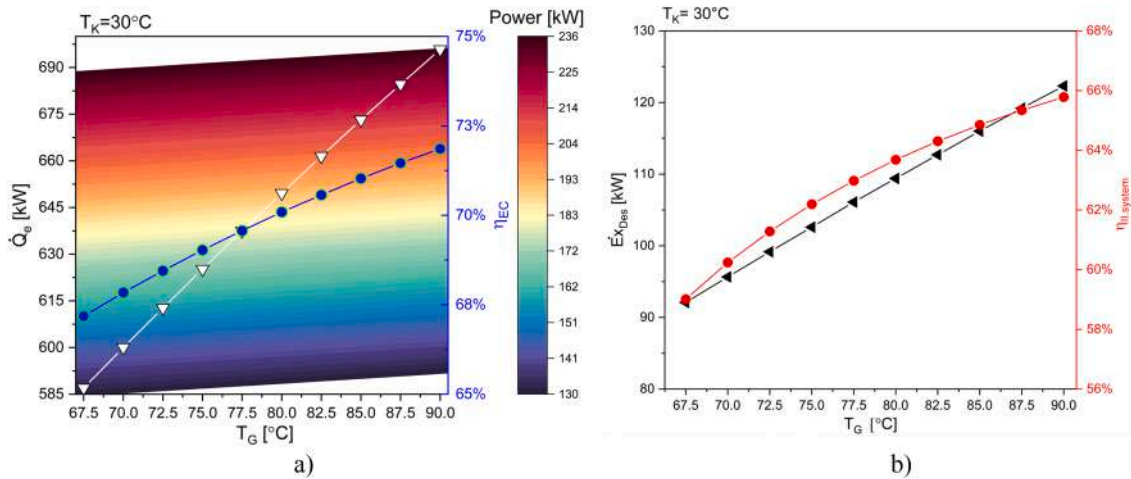**Fig. 10.** Effect of greenhouse temperature on overall system exergy performance.

Fig. 11. Effect of geothermal supply temperature on a) energy performance, b) exergy performance.

4.3. Energy performance comparison with conventional ORC and heat pump

This section compares the current system with the separated ORC and multi evaporator system (MES) (Fig. 12). Power generation and consumption are considered at the same operating conditions and cooling capacity.

As shown in Fig. 13.a, the ORCEMES increases power generation from 21% to 75% (at high and low geothermal temperatures, respectively). Moreover, environmentally friendly working fluids decrease direct CO_2e emissions due to lower GWP values than HFCs. The proposed CEMES reduces compressor power compression above 85% of that MES, leading to COP increase, Fig. 13.b. Therefore, combining both subsystems (ORC with CEMES) results in significant carbon footprint reductions.
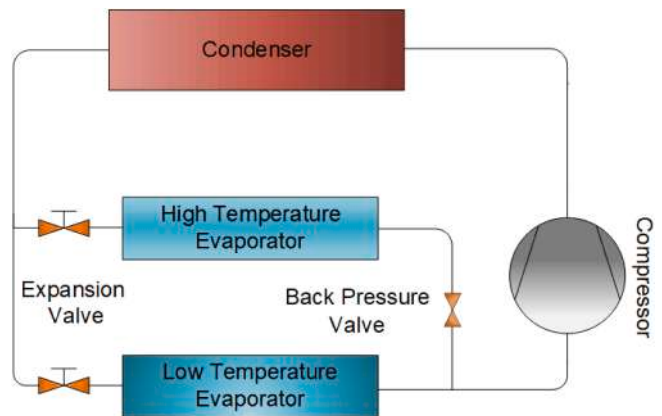

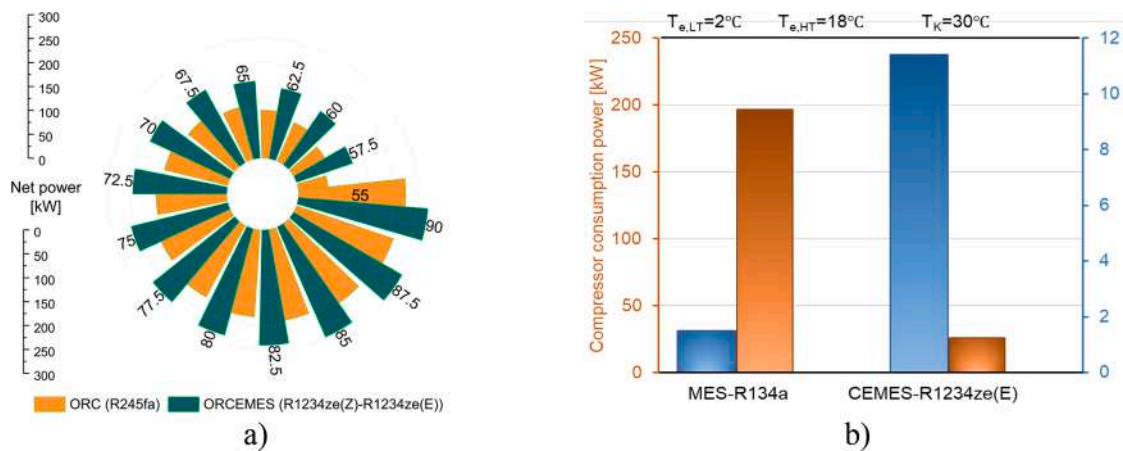**Fig. 12.** Multi-evaporators vapour compression cycle system (MES).

Fig. 13. (a). ORCEMES and ORC net power at different geothermal supply temperatures. (b). CEMES and MES power consumption and COP.

5. Conclusions

The current work analyses the energy and exergy performance of a combined organic Rankine and compound ejector-multi evaporator vapour compression system for two cooling levels and heating purposes with power generation, geothermal and condenser waste heat utilisation. The system is considered for two modes: power-cooling with condenser waste heat utilisation and power-heating. It includes six ultra-low GWP refrigerants (nine pairs of refrigerants). The main conclusions of the work are exposed in the following.

The novel arrangement shows the highest system COP using the working fluids R1234ze(E) and R1234ze(Z) as refrigerants pair in the power-cooling mode, with the highest power generation.

Because the compressor power consumption increase and turbine power generation decrease, the condensing temperature increase of each subsystem has the most detrimental effect on both net power generation and thermal efficiency at a given geothermal supply temperature. The highest system COP is obtained at 25 ℃ and 30 ℃ ORC and CEMES condensing temperature, respectively, for the analysed geothermal supply temperature range.

The increase in the greenhouse temperature augments the overall COP, with a modest increment in net power generation and thermal efficiency. The thermoeconomic efficiency slightly increases because of a smaller benefit in power generation and irreversibility. The power generation, thermal efficiency and overall system COP have followed the geothermal supply temperature.

In the exergy analysis, the low-temperature level recapture heat exchanger represents the highest source of exergy destruction, whereas the second expansion valve shows the lowest value. The exergy efficiency is directly proportional to the geothermal supply temperature for both modes.

Finally, compared with single ORC and multi evaporator systems, the proposed system increases power generation from 21% to 75% at high and low geothermal temperatures under the same conditions and cooling capacity. Additionally, the proposed CEMES reduces compressor power consumption to 85% of that multi evaporator system, benefitting COP.

CRediT authorship contribution statement

Ali Khalid Shaker Al-Sayyab: Conceptualization, Methodology, Software, Writing – original draft, Writing – review & editing. **Adrián Mota-Babiloni:** Conceptualization, Methodology, Writing – review & editing, Supervision. **Ángel Barragán-Cervera:** Writing – review & editing, Resources. **Joaquín Navarro-Esbrí:** Writing – review & editing, Supervision, Project administration, Funding acquisition.

Declaration of Competing Interest

The authors declare that they have no known competing financial interests or personal relationships that could have appeared to influence the work reported in this paper.

Acknowledgements

References

[1] Jarraud M, Steiner A. Climate Change 2014 Synthesis Report. 2015. https://doi.org/10.1017/CBO9781139177245.003.
[2] Severe-weather 2021. https://www.severe-weather.eu/europe-weather (accessed August 10, 2021).
[3] European Commission. 2030 Climate & Energy Framework. Report 2014:1–16.
[4] European Commission. Shedding light on energy in the EU - A guided tour of energy statistics. Eur Comm 2021;47:1–28.
[5] The International Renewable Energy Agency. Renewable Energy Prospects for the European Union. 2018.
[6] Pierce V. Introduction to Geothermal power. first edit. The English Press; 2011.
[7] Li J, Pei G, Ji J, Bai X, Li P, Xia L. Design of the ORC (organic Rankine cycle) condensation temperature with respect to the expander characteristics for domestic CHP (combined heat and power) applications. Energy 2014;77:579–90. https://doi.org/10.1016/j.energy.2014.09.039.
[8] Meng N, Li T, Gao X, Liu Q, Li X, Gao H. Thermodynamic and techno-economic performance comparison of two-stage series organic Rankine cycle and organic Rankine flash cycle for geothermal power generation from hot dry rock. Appl Therm Eng 2022;200:117715. https://doi.org/10.1016/j.applthermaleng.2021.117715.
[9] UNEP. The Kigali Amendment to the Montreal Protocol: HFC Phase-down. OzonAction Fact Sheet 2016:1–7.
[10] Le VL, Feidt M, Kheiri A, Pelloux-Prayer S. Performance optimisation of low-temperature power generation by supercritical ORCs (organic Rankine cycles) using low GWP (global warming potential) working fluids. Energy 2014;67:513–26. https://doi.org/10.1016/j.energy.2013.12.027.
[11] Ministry of Development. Update of the Long-Term Strategy for Energy Renovation in the Building Sector in Spain 2017:73.
[12] Aphornratana S, Sriveerakul T. Analysis of a combined Rankine-vapour-compression refrigeration cycle. Energy Convers Manag 2010;51:2557–64. https://doi.org/10.1016/j.enconman.2010.04.016.
[13] Zhao Y, Wang J, Cao L, Wang Y. Comprehensive analysis and parametric optimisation of a CCP (combined cooling and power) system driven by geothermal source. Energy 2016;97:470–87. https://doi.org/10.1016/j.energy.2016.01.003.
[14] Saleh B. Energy and exergy analysis of an integrated organic Rankine cycle-vapor compression refrigeration system. Appl Therm Eng 2018;141:697–710. https://doi.org/10.1016/j.applthermaleng.2018.06.018.
[15] Liao G, Liu L, Zhang F, Jiaqiang E, Chen J. A novel combined cooling-heating and power (CCHP) system integrated organic Rankine cycle for waste heat recovery of bottom slag in coal-fired plants. Energy Convers Manag 2019;186:380–92. https://doi.org/10.1016/j.enconman.2019.02.072.

[16] Zhar R, Allouhi A, Ghodbane M, Jamil A, Lahrech K. Parametric analysis and multi-objective optimisation of a combined Organic Rankine Cycle and Vapor Compression Cycle. Sustain Energy Technol Assessments 2021;47:101401. https://doi.org/10.1016/j.seta.2021.101401.

[17] Lu F, Zhu Y, Pan M, Li C, Yin J, Huang F. Thermodynamic, economic, and environmental analysis of new combined power and space cooling system for waste heat recovery in waste-to-energy plant. Energy Convers Manag 2020;226:113511. https://doi.org/10.1016/j.enconman.2020.113511.

[18] Bao J, Zhang L, Song C, Zhang N, Zhang X, He G. Comparative study of combined organic Rankine cycle and vapor compression cycle for refrigeration: Single fluid or dual fluid? Sustain Energy Technol Assessments 2020;37:100595. https://doi.org/10.1016/j.seta.2019.100595.

[19] Zhu Y, Li W, Wang Y, Li H, Li S. Thermodynamic analysis and parametric optimisation of ejector heat pump integrated with organic Rankine cycle combined cooling, heating and power system using zeotropic mixtures. Appl Therm Eng 2021;194:117097. https://doi.org/10.1016/j.applthermaleng.2021.117097.

[20] Akrami E, Chitsaz A, Ghamari P, Mahmoudi SMS. Energy and exergy evaluation of a tri-generation system driven by the geothermal energy. J Mech Sci Technol 2017; 31:401–8. https://doi.org/10.1007/s12206-016-1242-y.

[21] Boyaghchi FA, Chavoshi M. Multi-criteria optimisation of a micro solar-geothermal CCHP system applying water/CuO nanofluid based on exergy, exergoeconomic and exergoenvironmental concepts. Appl Therm Eng 2017;112:660–75. https://doi.org/10.1016/j.applthermaleng.2016.10.139.

[22] Li B, Wang S-S, Wang K, Song L. Thermo-economic analysis of a combined cooling, heating and power system based on carbon dioxide power cycle and absorption chiller for waste heat recovery of gas turbine. Energy Convers Manag 2020;224: 113372.

[23] Nasir MT, Ekwonu MC, Esfahani JA, Kim KC. Performance assessment and multi-objective optimisation of an organic Rankine cycles and vapor compression cycle based combined cooling, heating, and power system. Sustain Energy Technol Assessments 2021;47:101457. https://doi.org/10.1016/j.seta.2021.101457.

[24] Teng S, Feng YQ, Hung TC, Xi H. Multi-objective optimisation and fluid selection of different cogeneration of heat and power systems based on organic rankine cycle. Energies 2021;14. https://doi.org/10.3390/en14164967.

[25] Aliahmadi M, Moosavi A, Sadrhosseini H. Multi-objective optimisation of regenerative ORC system integrated with thermoelectric generators for low-temperature waste heat recovery. Energy Rep 2021;7:300–13. https://doi.org/10.1016/j.egyr.2020.12.035.

[26] Al-Sayyab AKS, Navarro-Esbrí J, Mota-Babiloni A. Energy, exergy, and environmental (3E) analysis of a compound ejector-heat pump with low GWP refrigerants for simultaneous data center cooling and district heating. Int J Refrig 2022;133:61–72.

[27] S.A. Klein. Engineering Equation Solver 2019.

[28] ASHRAE. Standard 34,designation and safety classification of refrigerants. 2019.

[29] Colmenar-Santos A, Folch-Calvo M, Rosales-Asensio E, Borge-Diez D. The geothermal potential in Spain. Renew Sustain Energy Rev 2016;56:865–86. https://doi.org/10.1016/j.rser.2015.11.070.

[30] Xue X-D, Zhang T, Zhang X-L, Ma L-R, He Y-L, Li M-J, et al. Performance evaluation and exergy analysis of a novel combined cooling, heating and power (CCHP) system based on liquid air energy storage. Energy 2021;222:119975. https://doi.org/10.1016/j.energy.2021.119975.

[31] Liu X, Fu R, Wang Z, Lin L, Sun Z, Li X. Thermodynamic analysis of transcritical CO2 refrigeration cycle integrated with thermoelectric subcooler and ejector. Energy Convers Manag 2019;188:354–65. https://doi.org/10.1016/j.enconman.2019.02.088.

[32] Molés F, Navarro-Esbrí J, Peris B, Mota-Babiloni A, Kontomaris K. Thermodynamic analysis of a combined organic Rankine cycle and vapor compression cycle system activated with low temperature heat sources using low GWP fluids. Appl Therm Eng 2015;87:444–53. https://doi.org/10.1016/j.applthermaleng.2015.04.083.

[33] Khalid Shaker Al-Sayyab A, Mota-Babiloni A, Navarro-Esbrí J. Novel compound waste heat-solar driven ejector-compression heat pump for simultaneous cooling and heating using environmentally friendly refrigerants. Energy Convers Manage 2021;228:113703.

[34] Ashwni, Sherwani AF, Tiwari D. Exergy, economic and environmental analysis of organic Rankine cycle based vapor compression refrigeration system. Int J Refrig 2021;126:259–71.

[35] T.J. Kotas. The Exergy Method of Thermal Plant Analysis. Elsevier; 1985. https://doi.org/10.1016/C2013-0-00894-8.

[36] Li Z, Li W, Xu B. Optimization of mixed working fluids for a novel trigeneration system based on organic Rankine cycle installed with heat pumps. Appl Therm Eng 2016;94:754–62. https://doi.org/10.1016/j.applthermaleng.2015.10.145.

[37] Al-Sayyab AKS, Abdulwahid MA. Energy-exergy analysis of multistage refrigeration system and flash gas intercooler working with ozone-friendly alternative refrigerants to R134a. J Adv Res Fluid Mech Therm Sci 2019;63: 188–98. https://www.akademiabaru.com/submit/index.php/arfmts/article/view/2730/1791.

[38] Al-Sayyab AKS, Navarro-Esbrí J, Soto-Francés VM, Mota-Babiloni A. Conventional and advanced exergoeconomic analysis of a compound ejector-heat pump for simultaneous cooling and heating. Energies 2021;14(12):3511.